

MGFFD-VLM: Multi-Granularity Prompt Learning for Face Forgery Detection with VLM

Tao Chen, Jingyi Zhang, Decheng Liu, Chunlei Peng

Abstract

Recent studies have utilized visual large language models (VLMs) to answer not only "Is this face a forgery?" but also "Why is the face a forgery?" These studies introduced forgery-related attributes, such as forgery location and type, to construct deepfake VQA datasets and train VLMs, achieving high accuracy while providing human-understandable explanatory text descriptions. However, these methods still have limitations. For example, they do not fully leverage face quality-related attributes, which are often abnormal in forged faces, and they lack effective training strategies for forgery-aware VLMs. In this paper, we extend the VQA dataset to create DD-VQA+, which features a richer set of attributes and a more diverse range of samples. Furthermore, we introduce a novel forgery detection framework, MGFFD-VLM, which integrates an Attribute-Driven Hybrid LoRA Strategy to enhance the capabilities of Visual Large Language Models (VLMs). Additionally, our framework incorporates Multi-Granularity Prompt Learning and a Forgery-Aware Training Strategy. By transforming classification and forgery segmentation results into prompts, our method not only improves forgery classification but also enhances interpretability. To further boost detection performance, we design multiple forgery-related auxiliary losses. Experimental results demonstrate that our approach surpasses existing methods in both text-based forgery judgment and analysis, achieving superior accuracy.

Introduction

Face forgery detection refers to distinguishing real faces from forgery faces through deep learning methods. With the increasingly mature development of AGI nowadays, most people cannot distinguish between real and forgery faces. Therefore, face forgery detection is currently a research hotspot and plays an important role in fields such as social security and economic security.

Existing face forgery detection models typically employ binary classification networks and leverage techniques like data augmentation, frequency analysis, and temporal analysis to improve performance. Although these models demonstrate excellent accuracy on classification metrics, they lack interpretability and fail to explain the basis of authenticity judgments. Although saliency maps are a commonly used interpretability method, they can only show the decision-making regions and cannot explain why these regions are

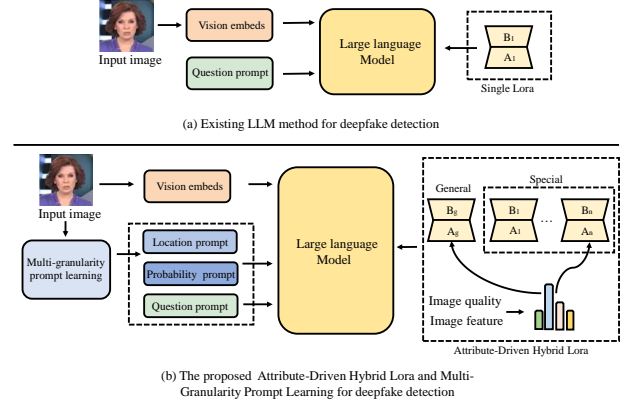


Figure 1: This figure illustrates the distinctions between our approach and the existing LLM method for deepfake detection. We employ attribute-driven hybrid LoRA strategy and multi-granularity prompt learning to enhance the accuracy and interpretability of forgery explanations.

selected. Beyond simply providing numerical predictions, understanding *why* a face is identified as fake is crucial for developing robust face forgery detection systems.

To access this need, Zhang *et al.* (Zhang *et al.* 2024) introduced a forgery VQA dataset (DD-VQA) based on human face perception and trained a question-answering visual large language model on this dataset to provide explanations for forgery detection. This approach has significantly advanced progress in the field. However, these approaches still have two limitations: (1) Existing deepfake VQA datasets, despite their benefits, rely on manually annotated data. This limits their diversity and fails to account for other deepfake-related facial features, such as abnormal quality, clarity, visibility, and illumination, which often appear abnormal in forged faces. (2) Given that forgery clues are often imperceptible, it is highly challenging to effectively guide large-scale visual-language models to focus on forgery-specific features.

To address the issue (1), we augment the text pair generation methods for Forgery Area and Forgery Type, which can be generated in a self-supervised manner based on DD-VQA. Meanwhile, we introduce additional facial features re-

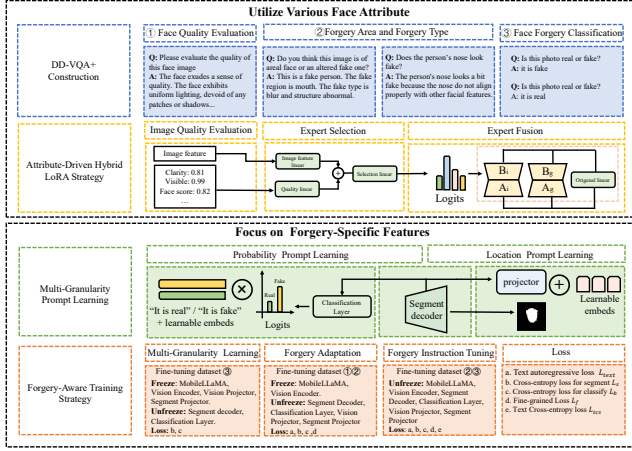


Figure 2: The overview of proposed MGFFD-VLM framework.

lated to forgery detection to enhance diversity. Additionally, during the training process of large language models, we propose an Attribute-driven Hybrid LoRA Strategy to boost the performance of Visual Large Language Models (VLMs). As shown in Figure 1, each sample selects an appropriate LoRA expert based on the current image quality and text characteristics, thus improving the detection capabilities in the varying image qualities. **To address the issue (2),** we employ multi-granularity prompts to guide the model in capturing forgery-related details at various levels. As illustrated in Figure 1, this approach converts classification and forgery segmentation results into prompts. To further enhance the model’s capability, in the Forgery-Aware Training Strategy, we introduce fine-grained image contrast losses and apply a soft-label cross-entropy loss at specific word prediction locations, thereby increasing the semantic distance between real and fake representations. The primary contributions of our work are as follows:

- This paper introduces DD-VQA+, an enhanced version of DD-VQA, integrating forgery classification, localization, forgery-related attributes, and human-perceptible explanations. We supplement Forgery Area and Forgery Type, which can self-supervise the generation of forgery locations and attributes. Meanwhile, we introduce additional face quality-related attributes.
- We propose Multi-Granularity Prompt Learning, enabling the VLM to leverage classification and forgery segmentation outputs as prompts, thereby enhancing both detection accuracy and model interpretability.
- We propose an Attribute-driven Hybrid LoRA Strategy. Specifically, we dynamically select suitable LoRA experts based on image quality attributes and image features, thereby effectively analyzing forged images with varying attributes.
- We propose Forgery-Aware Training Strategy. Increase the perception ability of forgery cues through a progressive learning strategy and carefully designed loss functions.



Figure 3: Demonstration of blend image generation in DD-VQA+ Construction. Random parts of real photos are replaced by fake faces.

Methodology

Figure 2 provides an overview of the proposed **MGFFD-VLM** framework. Our approach has two major components: (i) better use of facial image attributes through an extended dataset and an attribute-driven LoRA design, and (ii) enhanced forgery-aware learning through multi-granularity prompts and a specialized training strategy. In the following, we first briefly introduce our base model (MobileVLM), then describe the construction of DD-VQA+, and finally detail our prompt learning, hybrid LoRA, and training strategy.

Mobile-VLM

We use Mobile-VLM, proposed by the Meituan team, as our baseline model. As shown in the lower part of Figure 4, this model is primarily composed of three components: the Vision Encoder based on ViT-L/14, the Lightweight Downsample Projector, and the 1.4B parameter MobileLLaMA large language model. The Lightweight Downsample Projector, introduced by the Meituan team, significantly reduces the computational load, making it an efficient projector. Despite having only 1.7B parameters in total, this model achieves performance comparable to that of much larger models. Meanwhile, their training strategy consists of two stages. In the first stage, only the projector is unlocked, while in the second stage, fine-tuning of the large language model is carried out simultaneously. For MobileVLM, it has inputs (A, P, X) , where A is the expected answer, P is the asked question, and X is the corresponding image. The model mainly extracts image features through ViT and maps the image features to the text space through a projector. Then, the question prompt $P_{question}$ and the visual embeds P_{vision} are input into the LLM together for prediction.

DD-VQA+ Construction

Zhang *et al.* (Zhang et al. 2024) introduced a visual question answering (VQA) dataset for forgery detection, known as DD-VQA, which incorporates both common forgery questions Q_{common} and annotated answers A_{common} . The question Q_{common} prompts the model to evaluate whether specific facial features (such as the entire face, eyes, nose and mouth) appear fake in the image. All responses, A_{common} , are manually annotated. Their work demonstrated that manually annotated forgery locations and attributes can significantly improve the effectiveness of forgery detection, marking a major advancement in interpretable face forgery detection. However, due to the limited scale of DD-VQA, we supplemented Forgery Area and Forgery Type, which can generate forgery locations and attributes in a self-supervised

method. Meanwhile, we argue that incorporating additional face quality-related attributes can further enhance VLMs' confidence in forgery judgment. We introduce more additional facial attributes related to face forgery detection in the Face Quality Evaluation. We extend DD-VQA to DD-VQA+ by incorporating the key facial attributes mentioned above. Specifically, we introduce three new attributes, which are described in detail below:

Forgery Regions and Forgery Types. Accurately locating the forged areas can help large models better understand the concept of forgery. we supplement Forgery Area and Forgery Type, which can generate forgery locations and attributes in a self-supervised. Following the approach of Sun *et al.* (Sun et al. 2023), we create blended images by replacing parts of real images with altered, fake segments, as illustrated in Figure 3. For a forgery image x_i , we use the following formula:

$$x_i^{blend} = M_i \times x_i^{real} + (1 - M_i) \times x_i. \quad (1)$$

M_i is a binary mask that includes one of the following: the mouth, the nose, the eyes, or the entire face, and x_i^{real} represents the original image corresponding to x_i . Unlike the original text, we randomly select regions instead of choosing the regions with the largest differences. The standardized query Q_{local} is defined as "Do you think this image is of a real face or an altered fake one?" The model's answer begins with the fixed statement T_{label} , "This is an example of a fake face", followed by details on the specific forgery area and type. For real faces, the model simply responds with "It is a real face." The response, A_{local} , can be composed of the following elements:

$$A_{local} = T_{label} + T_{region} + T_{type}. \quad (2)$$

We predefine distinct text descriptions T_{region} for each replaced part. There are five types of T_{type} in total, namely blur, structure abnormal, color difference, and blend boundary (details can be found in (Sun et al. 2023)).

Face Quality Evaluation. Since generative algorithms often neglect the consistency of illumination intensity and facial visibility, forged faces may exhibit abnormalities in these attributes. To address this, we propose quantifying face quality indicators. The standardized prompt, $Q_{quality}$, is defined as "Please evaluate the quality of this face image." The model is then tasked with assessing the visual quality of the image from several perspectives, including overall impression, facial integrity, illumination intensity, illumination uniformity, clarity, and visibility. The response, $A_{quality}$, can be composed of the following components:

$$A_{quality} = T_{overall} + T_{face} + T_{intensity} + T_{uniformity} + T_{clarity} + T_{visibility}. \quad (3)$$

In this formula, each $T_{[\cdot]}$ represents a randomly chosen textual description corresponding to a specific aspect. Taking $T_{visibility}$ as an example, we first use the CPBD (Narvekar and Karam 2011) metric to calculate the scores that indicate the face's visibility. These scores are then categorized into three levels, with corresponding prompts such as "The facial visibility is high/mid/low." To

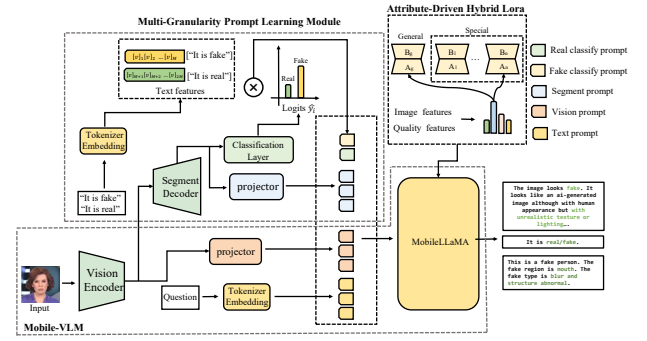


Figure 4: The overview of proposed Multi-Granularity Prompt Learning.

ensure prompt diversity, we use GPT-4 to generate 50 synonymous sentences with similar meanings. Finally, one sentence is randomly selected based on the score level. For example, when the CPBD score is 0.9, the generated prompt $T_{visibility}$ will be "The face is clearly visible." For the illumination factor $T_{intensity}$, we follow a similar approach to the method in (Ou et al. 2024) by training a CNN on the WIDER FACE dataset (Yang et al. 2016) to determine the illumination score. Like $T_{visibility}$, the score is divided into three levels, and GPT-4 is used to expand the text prompts. If $T_{intensity}$ is less than 0.3, the prompt will be set to "The brightness level on the face is dim." Further details can be found in the supplementary material.

Face Forgery Classification. Additionally, we develop Face Forgery Classification attributes. Here, forgery judgment texts are generated in a self-supervised manner based on classification labels. The standardized prompt is "Is this image real or fake?", with corresponding answers provided for real and fake images, respectively.

For x_i , we can obtain:

$$\begin{cases} Q_i = \{Q_{local}^i, Q_{common}^i, Q_{classify}^i, Q_{quality}^i\} \\ A_i = \{A_{local}^i, A_{common}^i, A_{classify}^i, A_{quality}^i\} \end{cases}. \quad (4)$$

Here, Q_i and A_i are generated by randomly selecting elements from predefined lists according to the above formulas, enabling us to capture a broad range of characteristics and responses related to the input x_i .

Multi-Granularity Prompt Learning

Existing visual large language models (VLMs) lack visual prompts that are directly applicable to face forgery detection. To make the model focus more on forgery-related features, we introduce Multi-Granularity Prompt Learning to enhance both the accuracy and interpretability of forgery detection. As shown in Figures 4, our proposed prompt learning framework consists of two key components: the Probability Prompt and the Location Prompt. The Probability Prompt is generated by integrating binary classification logits with the corresponding text embeddings, while the Location Prompt is mapped to the text feature space via a pro-

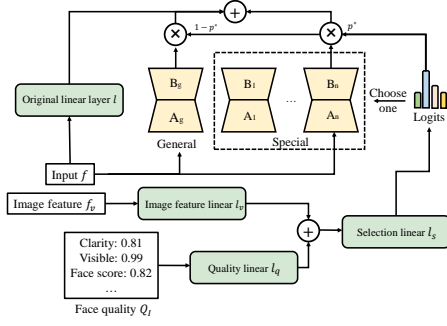


Figure 5: Illustration of the Attribute-Driven Hybrid LoRA Strategy.

jector, allowing it to capture spatial forgery cues more effectively.

Probability Prompt Learning. We begin by extracting image features using the vision encoder, which are then passed to the segmentation decoder. We use the simple DeepLabv3 Decoder (Yurtkulu, Şahin, and Unal 2019) as our segment Decoder. The segmentation features from the last layer are fed into a linear head to produce the binary classification result, denoted as \hat{y}_i . Following the approach of CoOp (Zhou et al. 2022), we define the corresponding text embeddings as follows:

$$\begin{cases} P_{fake} = [V]_1[V]_2 \dots [V]_M [\text{it is fake}] \\ P_{real} = [V]_{M+1}[V]_{M+2} \dots [V]_{2M} [\text{it is real}] \end{cases} \quad (5)$$

Each $[V]_m$ ($m \in [1, 2, \dots, 2M]$) is a vector matching the word embedding dimension. $[\text{it is real}]$ and $[\text{it is fake}]$ are the associated text embeddings. We calculate the Probability Prompt as follows:

$$P_i^{probability} = F_{concat}([\hat{y}_i \times P_{fake}, (1 - \hat{y}_i) \times P_{real}]). \quad (6)$$

The higher the value of \hat{y}_i , the easier it is for the large language model to understand the prompt $[\text{it is fake}]$. Conversely, the lower the value of \hat{y}_i , the easier it is for the large language model to understand the prompt $[\text{it is real}]$.

Location Prompt Learning. To capture spatial forgery details, we obtain the segmentation feature from the last layer of the segmentation decoder. Then, through a projector, it is mapped to the feature space of the text, and we refer to this feature as t_i^s , where the shape of t_i^s is $L \times D$. Finally, t_i^s is combined with L learnable vectors for enhanced expressiveness:

$$P_i^{segment} = t_i^s + [V]_{2M+1}[V]_{2M+2} \dots [V]_{2M+L}. \quad (7)$$

Here, M, H are hyperparameters, and D is the feature dimension. In addition, the LLM input includes visual embeddings P_i^{vision} aligned by projector. Thus, the final LLM input P_i^{all} incorporates the visual embeddings, question prompt, and both the probability and location prompts:

$$P_i^{all} = \{P_i^{probability}, P_i^{segment}, P_i^{question}, P_i^{vision}\}. \quad (8)$$

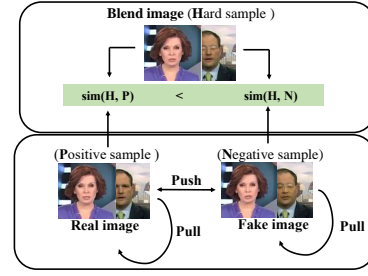


Figure 6: Illustration of the Fine-grained loss. P represents Real image, N represents Fake image, and H represents Blend image. We use $\text{sim}(\cdot)$ to represent the cosine similarity between samples.

Attribute-Driven Hybrid LoRA Strategy

While face quality doesn't directly indicate forgery, it influences how artifacts appear. Our LoRA uses specialized experts to focus on different signals (e.g., high-frequency details or compression artifacts). Inspired by (Wu, Huang, and Wei 2023), we propose an Attribute-Driven Hybrid LoRA Strategy that allows large models to focus on face quality scores while performing tampering-related question-answering tasks. As illustrated in Fig. 5, the process begins by employing a pre-trained image quality model M_q to extract a set of numerical quality indicators Q_I for each input image x . These indicators are analogous to those used in standard Face Quality Evaluation.

For each original linear layer l within the large language model, let the input feature from the previous layer be denoted as f . This feature f_v from vision encoder is processed by a image feature linear layer l_v , which produces a feature-based selection representation v_s . In parallel, the quality indicators Q_I is transformed into a quality-based selection representation q_s through a quality linear layer l_q . These two representations are then concatenated and passed through a selection linear layer l_s , resulting in a 4-dimensional vector. After applying softmax normalization, the resulting values represent the selection probabilities over the expert branches. The expert corresponding to the highest probability is chosen to process the input feature f .

The final output of the hybrid LoRA module is computed as a weighted combination of the selected specific expert e_* (from a set of four specialized LoRA branches) and a global expert e_g . Specifically, the updated output feature f' for the current layer l is calculated as:

$$f' = p^* \cdot A_* B_*(f) + (1 - p^*) \cdot A_g B_g(f) + l(f)$$

where p^* is the highest expert selection probability, A_*, B_* are the adaptation matrices of the selected specific expert, and A_g, B_g are those of the global expert. The original linear transformation $l(f)$ is also incorporated via residual connection. The resulting output f' is then propagated to the next layer. Further implementation details are provided in the Supplementary Materials.

Table 1: We present experimental results from fine-tuning BLIP and BLIP-TI with the DD-VQA dataset, and Mobile-VLM and MGFFD-VLM with the extended DD-VQA+ dataset. Text accuracy and answer generation performance are reported for all four models. As our analysis relies on identifying the terms "real" or "fake" within the text, AUC scores are not provided. In this comparison, BLIP and BLIP-TI represent current state-of-the-art methods, Mobile-VLM serves as the baseline for DD-VQA+, and MGFFD-VLM is our proposed approach. The best results are shown in bold numbers.

Method	Dataset	Deepfake Detection				Answer Generation				
		Acc \uparrow	Recall \uparrow	Precision \uparrow	F1 \uparrow	BLUE-4 \uparrow	CIDEr \uparrow	ROUGE_L \uparrow	METEOR \uparrow	SPICE \uparrow
BLIP (Li et al. 2022)	DD-VQA	0.8168	0.9596	0.7861	0.8642	0.3569	1.8177	0.5664	0.3301	0.6658
BLIP-TI (Zhang et al. 2024)	DD-VQA	0.8749	0.9341	0.8697	0.9007	0.4075	2.0567	0.6085	0.3463	0.6915
Mobile-VLM (Chu et al. 2023)	DD-VQA	0.7699	0.7844	0.9081	0.8417	0.5202	3.0743	0.6778	0.3879	0.6544
Mobile-VLM	DD-VQA+	0.8802	0.9451	0.9055	0.9249	0.5308	3.1776	0.6840	0.3922	0.6599
MGFFD-VLM	DD-VQA+	0.9072	0.9619	0.9228	0.9420	0.5349	3.3008	0.6963	0.3988	0.6629

Table 2: The performance of multi-modal enhanced deepfake detection. We report the AUC (%). For the specially annotated "video," it represents the video-level result, while "frame" represents the frame-level result.

Method	Multi-modal Enhancement	Celeb-DF		DFDC	WDF
		Frame	Video	Frame	Frame
Xception (Chollet 2017)	X	61.80	-	64.05	62.72
Xception + PCC (Hua et al. 2023)	X	54.87	-	62.73	-
Xception + hierarchical (Yu et al. 2024)	X	72.86	-	69.23	-
Xception	BLIP-TI	64.30	-	-	64.53
Xception	MGFFD-VLM	74.78	-	77.03	77.84
RECCE (Cao et al. 2022)	X	68.71	-	62.41	64.31
RECCE	BLIP-TI	70.21	-	-	69.46
RECCE	MGFFD-VLM	70.77	-	72.67	74.38
SBI (Shiohara and Yamasaki 2022)	X	86.12	93.18	74.44	70.27
SBI	BLIP-TI	-	93.98	-	-
SBI	MGFFD-VLM	87.80	93.53	81.77	81.05

Forgery-Aware Training Strategy

Training a VLM to detect subtle forgeries and explain them requires careful strategy. We employ a three-stage **forgery-aware training** scheme along with multiple loss functions to progressively tune the model:

Stage 1: Multi-Granular Visual Learning. In the first stage, we focus on training the vision-side components for forgery detection. We freeze the LLM and train the segmentation decoder and the binary classification head using supervised signals from the images. We apply a binary cross-entropy loss L_b on the image-level real/fake prediction \hat{y}_i (using the ground truth label y_i), and a pixel-wise cross-entropy loss L_s on the segmentation map \hat{s}_i (using the ground-truth mask s_i of manipulated regions, when available). For the blended images we generated, the ground-truth mask is the region that was replaced. Through L_b and L_s , the model learns both coarse (image-level) and fine (pixel-level) features that distinguish fake content.

Stage 2: Forgery Adaptation with Prompts. In the second stage, we unfreeze the image projector and the prompt-related parameters (the learnable prompt embeddings and the projector for the segmentation features). The LLM remains frozen. We now introduce the multi-granularity prompts and train the model to align these prompts with the textual answers. At this stage, we include all types of Q&A from DD-VQA+ (common forgery questions, region/type, quality, etc.), so the prompt generation modules learn to assist in answering them correctly.

We also introduce a *fine-grained contrastive loss* L_f to reinforce the separation between real and fake in the feature space. As illustrated in Figure 6, we treat a partially fake

(blended) image as a hard positive example that should be closer to fully fake images than to real ones in the representation space. We form triplets consisting of a real image P , a fake image N , and a blended image H (which contains some fake content). Let $\text{sim}(a, b)$ denote the cosine similarity between features of images a and b . We impose:

$$L_f = -\log \frac{\exp(\text{sim}(N, H))}{\exp(\text{sim}(N, H)) + \exp(\text{sim}(P, H))},$$

along with standard terms to pull P closer to P and N closer to N (while pushing P away from N). This loss encourages H (the hard positive) to be more similar to N (fake) than it is to P (real), forcing the model to pick up even faint forgery cues in H . By the end of Stage 2, the visual encoder and prompt generators are well-aligned with forgery-related concepts, though the LLM itself has not yet been fine-tuned on these tasks.

Stage 3: Forgery Instruction Tuning. In the final stage, we fine-tune the entire VLM (the LLM is now trainable, augmented by our LoRA modules) on the QA tasks. We feed in the full prompts + image + question and train the model to generate the correct answer text. We use the standard autoregressive language modeling loss L_{text} on the answer sequences. Additionally, we introduce a *text calibration loss* L_{tcs} to ensure the model firmly distinguishes real vs fake in its textual output. Concretely, whenever the answer contains a phrase like It is a real (fake) face, we apply a binary cross-entropy on the logits of the word real vs fake at that position, using the ground truth label. This penalizes any ambiguity in the model’s choice of the authenticity word. By explicitly training the model on this classification word, we prevent it

from hedging (e.g., assigning high probability to both real and fake) and thus obtain clearer decisions in the generated explanations.

Through these three stages, our model first learns to extract and localize forgery features, then learns to represent and prompt them for the language model, and finally learns to articulate the detection and explanation in natural language. The total loss $L = L_{text} + \lambda_1 L_b + \lambda_2 L_s + \lambda_3 L_f + \lambda_4 L_{tcs}$ (with λ coefficients to balance terms) is optimized over the entire training process (with each stage focusing on different subsets as described).

Experiments

Experimental Setup

Training Dataset. Our image training data mainly comes from FaceForensics++ (FF++) (Rossler et al. 2019). The text training data mainly includes the Deepfake Detection VQA dataset (DD-VQA (Zhang et al. 2024)), as well as three additional attributes generated by ourselves.

Evaluation Dataset. Following the settings of Zhang et al. (Zhang et al. 2024), we focus on two aspects of the text responses on DD-VQA: the classification performance of the text answers and the generation performance of the text generation. For text classification indicators, we evaluate under the Accuracy (Acc), Recall, Precision, and F1. For text answering indicators, following the settings in (Zhang et al. 2024), we evaluate metrics such as BLUE4 (Papineni et al. 2002), CIDEr (Vedantam, Lawrence Zitnick, and Parikh 2015), ROUGEL (Lin 2004), METEOR (Banerjee and Lavie 2005), and SPICE (Anderson et al. 2016). For evaluating our method enhanced deepfake detection methods, we choose several challenging face forgery datasets, namely Celeb-DF (Li et al. 2020), Deepfake Detection Challenge (DFDC) (Dolhansky et al. 2020), and Wilddeepfake (WDF) (Zi et al. 2020). We report the area under the receiver operating characteristic curve (AUC).

Implementation Details. We extract frames from each video and process face alignment. We resize all face images into 336×336 . Our proposed method is based on the MobileVLM (Chu et al. 2023). We use Adam optimizer to train the framework with betas of 0.9 and 0.995. We set the batch size rate to 64 for the first and second stages, and 48 for the third stage. We set the learning rate to $4e-5$ for the first and second stages, and $1e-6$ for the third stage. We set the rank and alpha of LoRA to 64 and 16 respectively, and the LoRA dropout rate to 0.05.

Results on the DD-VQA dataset

We fine-tune MobileVLM and our proposed MGFFD-VLM on DD-VQA+ dataset and provide results for both deepfake detection and answer generation. Our model can according to the template answer "it is real/fake" and provide the corresponding reasons. We conduct corresponding comparison experiments and ablation experiments to illustrate the role of our proposed DD-VQA+ and multi-granularity prompt learning. As shown in Table 1, Row#1 and Row#2 are the results of fine-tuning BLIP using the DD-VQA dataset, and on this basis, the contrastive loss between images and texts is

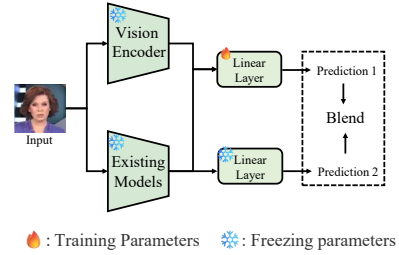


Figure 7: MGFFD-VLM Enhanced Deepfake Detection. We combine the vision features of the large model with the existing features

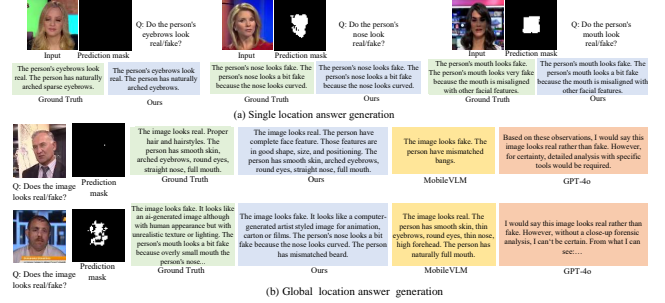


Figure 8: Results of Qualitative Examples.

added. Row#3 and Row#4 are both based on Mobile-VLM. The former uses DD-VQA while the latter uses DD-VQA+. It can be found that both have good performance in answer generation. However, due to the insufficient richness of DD-VQA+, in the deepfake detection task, using DD-VQA+ increases the Acc by 10% compared to DDVQA. Row#5 is based on Mobile-VLM. By adding the Probability prompt and Location prompt, it can be seen that the Acc of this method increases by more than 2%, and at the same time, the language ability also improves significantly.

Results on Deepfake Detection Models

As shown in Figure 7, we combine the vision features of the large model with the existing features to assess whether this fusion can enhance the effectiveness of existing models in forgery detection. We blend the output prediction from the small model (Prediction 1) with the fused result (Prediction 2) to obtain the final prediction. As shown in Table 2, we conduct experiments on three classic methods: Xception (Chollet 2017), RECCE (Cao et al. 2022) and SBI (Shiohara and Yamasaki 2022). For Xception, our method demonstrates significant improvement. Specifically, the detection auc improved by 12.98% on Celeb-DF, 12.98% on DFDC, and 15.12% on WDF. For RECCE, our method demonstrates significant improvement. Specifically, the detection auc improved by 2.06% on Celeb-DF, 10.26% on DFDC, and 10.07% on WDF. For SBI, the original paper primarily presents results at the video level. To ensure comparability, we first provide video-level detection results for Celeb-DF. Our method achieves a significantly higher improvement of 0.35%. Additionally, we report frame-level re-

Table 3: We present ablation experimental results for Multi-Granularity Prompt. The best results are shown in bold numbers. **Note:** FR+FT denotes Forgery Regions and Forgery Type; *Loc Prompt* represents Location Prompt; *Prob Prompt* stands for Probability Prompt. *ADH LoRA* stands for Attribute-Driven Hybrid LoRA Strategy.

DD-VQ+		Prompt Compents		Deepfake Detection				Answer Generation				
FR+FT	ADH LoRA	Loc Prompt	Prob Prompt	Acc \uparrow	Recall \uparrow	Precision \uparrow	F1 \uparrow	BLUE-4 \uparrow	CIDEr \uparrow	ROUGE_L \uparrow	METEOR \uparrow	SPICE \uparrow
✓				0.8745	0.9260	0.9143	0.9201	0.5214	3.1439	0.6789	0.3891	0.6578
✓		✓		0.8802	0.9451	0.9055	0.9249	0.5308	3.1776	0.6840	0.3922	0.6599
✓		✓		0.8954	0.9427	0.9251	0.9343	0.5411	3.2872	0.6989	0.3959	0.6547
✓		✓	✓	0.9030	0.9636	0.9168	0.9396	0.5482	3.2380	0.6937	0.3973	0.6586
✓	✓	✓	✓	0.9072	0.9619	0.9228	0.9420	0.5349	3.3008	0.6963	0.3988	0.6629

Table 4: We present ablation experimental results for loss. The best results are shown in bold numbers.

L_f	L_{tes}	Deepfake Detection			
		Acc \uparrow	Recall \uparrow	Precision \uparrow	F1 \uparrow
		88.32	94.73	90.74	92.69
✓		89.22	95.11	91.48	93.26
✓	✓	90.64	95.92	92.41	94.13

sults for SBI on Celeb-DF, WDF, and DFDC. Our reproduced results align closely with the official values provided in the original study. Notably, our method shows considerable improvement on Celeb-DF and WDF, with a minor performance decline on DFDC. Overall, these results demonstrate that our proposed method effectively enhances the detection performance of existing deepfake detection models across multiple datasets.

Results of Ablation Experiments

To explore how the designed key modules affect model performance, we conducted ablation experiments.

Effect of Forgery Regions and Forgery Types. As shown in Table 3, Row#1 represents the baseline trained only with the DD-VQA dataset. Row#2 supplements Forgery Regions and Forgery Types on the basis of the baseline. Incorporating the online-generated forgery localization task significantly enhances both the detection and response capabilities of the VLM. This improvement is attributed to the task’s focus on fine-grained forgery areas, which helps the VLM better understand forgery-related features.

Effect of Multi-Granularity Prompt. As presented in Table 3, Row#3 and Row#4 are the experimental results of adding Location Prompt and Probability Prompt in sequence. Adding the Location Prompt increases accuracy by 1.52% over Row#2, along with comprehensive improvements in language metrics. This indicates that incorporating forgery-related prompts enhances the model’s response capabilities. With the addition of the Probability Prompt, accuracy increases by 0.76%, though improvements in answer generation are less noticeable since the Probability Prompt is primarily suited to classification tasks. This prompt has less impact when the model is asked to identify unnatural aspects in specific regions. Overall, adding both Location and Probability Prompts achieves the best performance.

Effect of Attribute-Driven Hybrid LoRA Strategy. As presented in Table 3, Row#5 are the experimental results of adding Attribute-Driven Hybrid LoRA Strategy. Our LoRA integration led to significant gains in numerical metrics (e.g.,

deepfake detection accuracy). Simultaneously, the performance of most text - related tasks also shows an enhancement. This improvement can be attributed to the selection of corresponding experts for photos of different qualities, which in turn enhances the detection capabilities. Regarding the ablation experiments between the image feature and the quality feature, please refer to the supplementary file for more details.

Effect of Fine-Grained Loss and Text Cross-entropy Loss. As shown in Table 4, Row#1 represents the MGFFD-VLM model without fine-grained loss and text cross-entropy loss during entire training phase. Row#2 builds upon the model of Row#1 by adding fine-grained loss, and Row#3 further enhances the model of Row#2 with the addition of text cross-entropy loss. when the fine-grained loss is added, the Acc of the model’s deepfake detection rises from 88.32% to 89.22%. This shows that our fine-grained loss can help the model learn fine-grained features that are difficult to mine. At the same time, after adding the Text cross-entropy loss, the Acc rises by 1.42%, indicating that multiple auxiliary losses can simultaneously promote forgery detection.

Qualitative results are provided in Figure 8. In these examples, our model accurately identifies fake faces and provides clear explanations (e.g., pointing out unnatural skin texture or odd facial blending in the fake images, or noting a completely natural appearance for a real image). In contrast, a generic large model (GPT-4) might only give a vague or guess-based answer, and the baseline MobileVLM without our enhancements often fails to pinpoint the issues. Our MGFFD-VLM can both detect the forgery and articulate the specific evidence, demonstrating the effectiveness of our approach.

Conclusion

We presented **MGFFD-VLM**, a vision-language framework for face forgery detection that produces both decisions and human-understandable explanations. By extending the training data (DD-VQA+) with richer forgery-related questions and by incorporating multi-granularity prompts, quality-aware LoRA experts, and a tailored training strategy, our model achieves state-of-the-art accuracy on deepfake detection while providing clear rationales. The results demonstrate the promise of using large VLMs for interpretable deepfake detection. In future work, we plan to explore further improvements in generalization to unseen manipulation methods.

References

- Anderson, P.; Fernando, B.; Johnson, M.; and Gould, S. 2016. Spice: Semantic propositional image caption evaluation. In *Computer Vision—ECCV 2016: 14th European Conference, Amsterdam, The Netherlands, October 11–14, 2016, Proceedings, Part V 14*, 382–398. Springer.
- Banerjee, S.; and Lavie, A. 2005. METEOR: An automatic metric for MT evaluation with improved correlation with human judgments. In *Proceedings of the acl workshop on intrinsic and extrinsic evaluation measures for machine translation and/or summarization*, 65–72.
- Cao, J.; Ma, C.; Yao, T.; Chen, S.; Ding, S.; and Yang, X. 2022. End-to-end reconstruction-classification learning for face forgery detection. In *Proceedings of the IEEE/CVF Conference on Computer Vision and Pattern Recognition*, 4113–4122.
- Chollet, F. 2017. Xception: Deep learning with depthwise separable convolutions. In *Proceedings of the IEEE conference on computer vision and pattern recognition*, 1251–1258.
- Chu, X.; Qiao, L.; Lin, X.; Xu, S.; Yang, Y.; Hu, Y.; Wei, F.; Zhang, X.; Zhang, B.; Wei, X.; et al. 2023. Mobilevlm: A fast, reproducible and strong vision language assistant for mobile devices. *arXiv preprint arXiv:2312.16886*.
- Dolhansky, B.; Bitton, J.; Pfau, B.; Lu, J.; Howes, R.; Wang, M.; and Ferrer, C. C. 2020. The deepfake detection challenge (dfdc) dataset. *arXiv preprint arXiv:2006.07397*.
- Hua, Y.; Shi, R.; Wang, P.; and Ge, S. 2023. Learning patch-channel correspondence for interpretable face forgery detection. *IEEE Transactions on Image Processing*, 32: 1668–1680.
- Li, J.; Li, D.; Xiong, C.; and Hoi, S. 2022. Blip: Bootstrapping language-image pre-training for unified vision-language understanding and generation. In *International conference on machine learning*, 12888–12900. PMLR.
- Li, Y.; Yang, X.; Sun, P.; Qi, H.; and Lyu, S. 2020. Celeb-df: A large-scale challenging dataset for deepfake forensics. In *Proceedings of the IEEE/CVF conference on computer vision and pattern recognition*, 3207–3216.
- Lin, C.-Y. 2004. Rouge: A package for automatic evaluation of summaries. In *Text summarization branches out*, 74–81.
- Narvekar, N. D.; and Karam, L. J. 2011. A no-reference image blur metric based on the cumulative probability of blur detection (CPBD). *IEEE Transactions on Image Processing*, 20(9): 2678–2683.
- Ou, F.-Z.; Li, C.; Wang, S.; and Kwong, S. 2024. CLIB-FIQA: Face Image Quality Assessment with Confidence Calibration. In *Proceedings of the IEEE/CVF Conference on Computer Vision and Pattern Recognition*, 1694–1704.
- Papineni, K.; Roukos, S.; Ward, T.; and Zhu, W.-J. 2002. Bleu: a method for automatic evaluation of machine translation. In *Proceedings of the 40th annual meeting of the Association for Computational Linguistics*, 311–318.
- Rossler, A.; Cozzolino, D.; Verdoliva, L.; Riess, C.; Thies, J.; and Nießner, M. 2019. Faceforensics++: Learning to detect manipulated facial images. In *Proceedings of the IEEE/CVF international conference on computer vision*, 1–11.
- Shiohara, K.; and Yamasaki, T. 2022. Detecting deepfakes with self-blended images. In *Proceedings of the IEEE/CVF Conference on Computer Vision and Pattern Recognition*, 18720–18729.
- Sun, K.; Chen, S.; Yao, T.; Yang, H.; Sun, X.; Ding, S.; and Ji, R. 2023. Towards general visual-linguistic face forgery detection. *arXiv preprint arXiv:2307.16545*.
- Vedantam, R.; Lawrence Zitnick, C.; and Parikh, D. 2015. Cider: Consensus-based image description evaluation. In *Proceedings of the IEEE conference on computer vision and pattern recognition*, 4566–4575.
- Wu, X.; Huang, S.; and Wei, F. 2023. Mole: Mixture of lora experts. In *The Twelfth International Conference on Learning Representations*.
- Yang, S.; Luo, P.; Loy, C.-C.; and Tang, X. 2016. Wider face: A face detection benchmark. In *Proceedings of the IEEE conference on computer vision and pattern recognition*, 5525–5533.
- Yu, B.; Li, W.; Li, X.; Zhou, J.; and Lu, J. 2024. Uncertainty-aware hierarchical labeling for face forgery detection. *Pattern Recognition*, 153: 110526.
- Yurtkulu, S. C.; Şahin, Y. H.; and Unal, G. 2019. Semantic segmentation with extended DeepLabv3 architecture. In *2019 27th Signal Processing and Communications Applications Conference (SIU)*, 1–4. IEEE.
- Zhang, Y.; Colman, B.; Shahriyari, A.; and Bharaj, G. 2024. Common Sense Reasoning for Deep Fake Detection. *arXiv preprint arXiv:2402.00126*.
- Zhou, K.; Yang, J.; Loy, C. C.; and Liu, Z. 2022. Learning to prompt for vision-language models. *International Journal of Computer Vision*, 130(9): 2337–2348.
- Zi, B.; Chang, M.; Chen, J.; Ma, X.; and Jiang, Y.-G. 2020. Wilddeepfake: A challenging real-world dataset for deepfake detection. In *Proceedings of the 28th ACM international conference on multimedia*, 2382–2390.